

EXACT FINITE DIFFERENCE SCHEMES FOR SOLVING HELMHOLTZ EQUATION AT ANY WAVENUMBER

YAU SHU WONG AND GUANGRUI LI

Abstract. In this study, we consider new finite difference schemes for solving the Helmholtz equation. Novel difference schemes which do not introduce truncation error are presented, consequently the exact solution for the Helmholtz equation can be computed numerically. The most important features of the new schemes are that while the resulting linear system has the same simple structure as those derived from the standard central difference method, the technique is capable of solving Helmholtz equation at any wavenumber without using a fine mesh. The proof of the uniqueness for the discretized Helmholtz equation is reported. The power of this technique is illustrated by comparing numerical solutions for solving one- and two-dimensional Helmholtz equations using the standard second-order central finite difference and the novel finite difference schemes.

Key words. Helmholtz equation, wavenumber, radiation boundary condition, finite difference schemes, exact numerical solution.

1. Introduction

The study of wave phenomena is important in many areas of science and engineering. The Helmholtz equation arises from time-harmonic wave propagation, and the solutions are frequently required in many applications such as aero-acoustic, underwater acoustics, electromagnetic wave scattering, and geophysical problems. Finite difference methods are commonly used to solve the Helmholtz equation. In addition to the standard central finite difference, Sutmann [16] derived a new compact finite difference scheme of sixth order for the Helmholtz equation and the convergence characteristics and accuracy were compared for a broad range of wavenumbers. Accurate high order finite difference methods were reported in Singer and Turkel [14, 15], Harari and Turkel [10]. A new nine-point sixth-order accurate compact finite-difference method for solving the Helmholtz equation in one and two dimensions was developed and analyzed in [13]. Other numerical techniques such as finite element and spectral methods have been applied to solve the problem. Babuška and Ihlenburg [11] used the h-version of the finite element method with piecewise linear approximation to solve a one-dimensional model problem, Babuška et al. [3] presented a systematic analysis of a posteriori estimation for finite element solutions. Harari and Magoulés [9] considered the Least-Squares stabilization of finite element computation for the Helmholtz equation. Babuška and Sauter [4] found that the solution of the Galerkin finite element method differs significantly from the best approximation with increasing wavenumber and claimed that it is impossible to eliminate the so-called pollution effect. A coupled finite-infinite element method was described, formulated and analyzed for parallel computations by Autrique and Magoulés [2]. Bao et. al. [5] considered the the pollution effect and explored the feasibility of a local spectral method, the discrete singular convolution algorithm for solving the Helmholtz equation with high wavenumbers. Recently, Gitteson et.

Received by the editors November 15, 2010.

2000 *Mathematics Subject Classification.* 65N06, 65N15, 65N22.

This work is supported by the Natural Sciences and Engineering Research Council of Canada.

al. [8] proposed discontinuous Galerkin finite element methods to capture the oscillatory behavior of the wave solution. It should be pointed out that all numerical methods require a very fine mesh in order to ensure the accuracy of the computed solutions at high wavenumbers.

The mathematical formulation for time harmonic wave propagation in the homogeneous media is given by the Helmholtz equation:

$$(1) \quad \Delta U + k^2 U = 0.$$

where $k = \omega/c$ denotes the wavenumber which is related to the frequency of the wave propagation ω and c is the speed of sound.

Even though tremendous progress has been reported in the areas of computational techniques for partial differential equations, solving a linear Helmholtz equation at high wavenumbers numerically remains as one of the most difficult tasks in scientific computing. At a high wavenumber, the solution of the Helmholtz equation is highly oscillatory. Suppose the mesh size of a numerical discretization is h , it has generally been recognized that to accurately capture the oscillatory behavior, it is necessary to require kh to be small. However, numerical simulation and theoretical study has confirmed that even when kh is fixed, the numerical accuracy deteriorates rapidly as k increases. This is known as the "pollution effect" [4]. The pollution error can only be eliminated completely for one-dimensional equation, and not for two- and three-dimensional problems. Moreover, to ensure an accurate numerical solution, it is essential to enforce the condition $k^2 h < 1$. However, this would imply that the number of the discretized equations is proportional to h^{-3} or k^3 . This will then lead to an extremely huge system of linear equations. It should be mentioned that the resulting system is highly indefinite for large wavenumbers, and many iterative techniques such as the conjugate gradient and multigrid methods are not capable of solving the indefinite systems.

Developing efficient and accurate numerical solutions for the Helmholtz equation at high wavenumbers is an active research topic. Although it has been reported in many engineering literatures that using 10 to 12 grid points per wavelength is sufficient to produce a reasonable accuracy for many problems, this general rule, however, can not be used when dealing with Helmholtz equation at highwave numbers.

In this paper, we consider a novel finite difference approach which satisfies exactly the interior points of the Helmholtz equation at any wavenumber. Using the same idea, we also derive the finite difference for the radiation boundary conditions. The most important result presented in this work is that the finite difference scheme is constructed so that the solution of the discretized equations satisfies the solution of the Helmholtz equation exactly at the interior grid points as well as the boundary. Since no discretization error is introduced, the numerical solution can be computed for all wavenumbers even if kh and $k^2 h$ is not small. Numerical simulations confirm that the new schemes produce exact numerical solution for one-dimensional problem. For a two-dimensional Helmholtz equation, accurate numerical solutions can be achieved even for the case $kh = 1.5$ and $k^2 h = 450$. To our knowledge, the exact finite difference scheme has not been reported and demonstrated for solving Helmholtz equation especially for applications to high wavenumbers.

The present study is organized as follows. In Section 2, we consider finite difference approximations for the Helmholtz equation. A novel difference approach is presented, so that the resulting difference equations satisfy exactly the original

continuous problem. The proof of uniqueness for the discrete problems are presented. Numerical simulations for one-dimensional and two-dimensional problems are reported in Section 3. Finally, we conclude the paper with a short remark in Section 4.

2. Finite difference schemes

In this section, we first recall the standard finite difference scheme, then we present the novel finite difference schemes for one- and two-dimensional Helmholtz equations.

2.1. One-dimensional problem. Consider a one-dimensional Helmholtz equation,

$$(2) \quad \begin{cases} -U_{xx} - k^2U = 0, & x \in (0, 1) \\ U(0) = 1, \\ U'(1) = ikU(1). \end{cases}$$

It should be note that in many applications dealing with wave scattering problems, the Helmholtz equation is defined in an unbounded physical domain. To avoid computation on infinite domain, artificial numerical boundary condition is commonly imposed so that the solution is sought in a finite computational domain. The artificial boundary condition (ABC) is constructed so that the nonphysical numerical reflection is eliminated or reduced in the computational domain. Sommerfeld's radiation condition can be considered as a first-order ABC, other high-order ABC schemes are studied by Engquist and Majda [7]. Berenger [6] reported the development of the perfectly matched layer method, and the approach has been applied to electromagnetic waves. For the model problems investigated in this paper, we consider Helmholtz equation with mixed boundary condition, in which a Dirichlet is given at one end and Sommerfeld's radiation condition is imposed at the other end. Similar models have been used in the study of numerical solution for the Helmholtz equation.

The simplest numerical discretization scheme is the use of the standard finite difference scheme, which can be derived by the Taylor's expansion. To approximate the first-order derivative, let δ_{0x} and δ_x denote the central difference operator and the backward difference operator, respectively. Using a straightforward Taylor's expansion, it can easily be verified that δ_{0x} is second-order accurate and δ_x is first-order accurate. Here,

$$\begin{aligned} \delta_{0x}U(x) &= \frac{U(x+h) - U(x-h)}{2h}, \\ \delta_xU(x) &= \frac{U(x) - U(x-h)}{h}, \end{aligned}$$

where h is the spatial step size.

Similarly, a central difference operator δ_x^2 for a second order derivative is second-order accurate, where

$$\delta_x^2U(x) = \frac{U(x+h) - 2U(x) + U(x-h)}{h^2}.$$

Now, applying the second order schemes for the Helmholtz equation and the boundary condition, we expect to have a second-order accurate numerical scheme $O(h^2)$ for the problem, and the truncation error is given by $c_1h^2 + c_2h^4 + c_3h^6 + \dots$, where c_i are constant. However, numerical simulations presented in the next section clearly indicate that the second-order accuracy is only achieved when the

wavenumber k and kh close to zero. Even when $kh = 0.5$, the standard difference scheme could produce enormous error when k is large.

It has already been accepted that solving Helmholtz equation at high wavenumbers is a difficult task. To the best of our knowledge, to ensure accurate numerical solutions, one would require k^2h to be small, but this will imply a very fine mesh is needed for large k . Consequently, considerable computing resource is needed to solve the resulting large system of equations. Is it possible to construct a numerical scheme such that the accuracy does not depend on kh and k^2h ? For the model equation consider in this paper, the answer is yes.

We now present a novel finite difference scheme for the Helmholtz equation proposed by Lambe et al. [12]. The scheme is developed by replacing the coefficient of $U(x)$ in the standard finite difference operator by a weight ω such that it minimizes

$$(3) \quad \left| U''(x) - \frac{U(x+h) - \omega U(x) + U(x-h)}{h^2} \right|.$$

It can be shown by Taylor's expansion that

$$(4) \quad U(x+h) + U(x-h) = 2[U(x) + u^{(2)}(x)\frac{h^2}{2!} + u^{(4)}(x)\frac{h^4}{4!} + \dots].$$

Hence, using the relation $U^{(2n)} = (-1)^n k^{2n} U$ for $n = 1, 2, \dots$ and the Taylor's series of $\cos(x)$, it gives

$$(5) \quad -k^2 U(x) = U''(x) = \frac{U(x+h) - \omega U(x) + U(x-h)}{h^2}.$$

Therefore, using $\omega = 2\cos(kh) + (kh)^2$, the new difference formula satisfies the equation exactly. Since there is no truncation error resulting from the numerical approximations, one would expect that it will produce exact numerical solution.

Unfortunately, this attractive finite difference scheme is not widely known in the computational science or engineering community. One of the reasons may be due to the fact that the major contribution of that paper was to illustrate the power of using symbolic computation to compute optimal weights which involve complicated manipulations with the integral formulas for two- and three-dimensional Helmholtz equations. While the new difference formula is exact for the interior points, there is no discussion on how to treat the boundary condition.

For the Sommerfeld's radiation boundary condition at $x = 1$, we have

$$(6) \quad U'(1) = ikU(1),$$

and the second-order accurate standard finite difference scheme with a truncation error $O(h^2)$ is given by

$$(7) \quad \frac{U(x+h) - U(x-h)}{2h} = ikU(x).$$

It will be demonstrated that although the solution at the interior points can be computed exactly using the new difference scheme, a numerical error at the boundary point can lead to an unacceptable solution for the problem at high wavenumbers. To ensure an accurate numerical solution, it is important to construct difference schemes which do not admit truncation errors at the interior points and at the boundary points.

By applying a similar idea presented in [12], we now develop a novel scheme for the radiation boundary condition $\frac{\partial U}{\partial x} = ikU$. From the Taylor's expansion, we have

$$U(x+h) = U(x) + hU'(x) + \frac{h^2}{2!}U''(x) + \frac{h^3}{3!}U^{(3)}(x) + \dots$$

$$U(x-h) = U(x) - hU'(x) + \frac{h^2}{2!}U''(x) - \frac{h^3}{3!}U^{(3)}(x) + \dots$$

Hence,

$$(8) \quad U(x+h) - U(x-h) = 2h(U'(x) + \frac{h^2}{3!}U^{(3)}(x)) + \frac{h^4}{5!}U^{(5)}(x) + \dots$$

By iterating the relation $\frac{\partial U}{\partial x} = ikU$, it follows that

$$(9) \quad \frac{\partial^n U}{\partial^n x} = (ik)^n U.$$

Substituting these values into equation (8), we obtain

$$(10) \quad \frac{U(x+h) - U(x-h)}{2h} = \frac{U'(x)}{kh} \sin(kh).$$

Thus, the new difference scheme for the radiation condition can be written as

$$(11) \quad U(x+h) - 2i \sin(kh)U(x) - U(x-h) = 0.$$

It is important to note that the novel boundary scheme has no truncation error and satisfies the radiation boundary condition exactly. Hence, for a one-dimensional Helmholtz equation considered here, the use of equations (5) and (11) produces exact numerical solution if the effect due to round-off error is ignored.

To prove the uniqueness of the resulting linear system using the new difference schemes, we first introduce the discretized integration by parts.

LEMMA 2.1 (Discretized integration by parts). *For any u_i and \bar{v}_i , $i = 0, 1, \dots, n+1$, we have*

$$(12) \quad -\sum_{i=1}^n \delta_x^2 u_i \bar{v}_i = \sum_{i=1}^n \delta_x u_i \delta_x \bar{v}_i - \frac{1}{h^2}(u_1 - u_0)\bar{v}_0 + \frac{1}{h^2}(u_{n+1} - u_n)\bar{v}_n$$

Proof: the proof is trivial.

THEOREM 2.1 (Uniqueness of the discretized solution). *By using the novel finite difference schemes, namely equation (5) and equation (11), the problem has a unique discretized solution.*

Proof: Assuming there are two solutions w and v , let $u = w - v$ then u satisfies the equation

$$(13) \quad \begin{cases} -\frac{u_{j+1} - \omega u_j + u_{j-1}}{h^2} - k^2 u_j = 0, & j = 1, 2, \dots, n \\ u_0 = 0 \\ u_{n+1} - 2i \sin(kh)u_n - u_{n-1} = 0. \end{cases}$$

Using Taylor's expansion for u_{n-1} and the relation (9), it yields

$$\begin{cases} -\delta_x^2 u_j - (\frac{2-\omega}{h^2} + k^2)u_j = 0, & j = 1, 2, \dots, n \\ u_0 = 0 \\ u_{n+1} - u_n = i \sin(kh)u_n - (1 - \cos(kh))u_n \end{cases}$$

By multiplying the equation by \bar{v}_j , then summing-up the equation for j from 1 to n and using the Lemma 2.1, we get

$$\sum_{j=1}^n \delta_x u_j \delta_x \bar{v}_j - \frac{1}{h^2}(u_1 - u_0)\bar{v}_0 + \frac{1}{h^2}(u_{n+1} - u_n)\bar{v}_n - \sum_{j=1}^n (\frac{2-\omega}{h^2} + k^2)u_j \bar{v}_j = 0$$

By the boundary condition, taking $\bar{v}_j = \bar{u}_j$ and noting $u_0 = 0$, we have

$$(14) \quad \sum_{j=1}^n \delta_x u_j \delta_x \bar{u}_j - \sum_{j=1}^n \left(\frac{2-\omega}{h^2} + k^2 \right) u_j \bar{u}_j - (1 - \cos(kh)) u_n \bar{u}_n + i \sin(kh) u_n \bar{u}_n = 0$$

Since the right-hand side of equation(14) is real, it follows that $u_n = 0$. Hence for any v_j , $j = 1, 2, \dots, n$,

$$(15) \quad \sum_{j=1}^n \delta_x u_j \delta_x \bar{v}_j = \sum_{j=1}^n \left(\frac{2-2\cos(kh)}{h^2} \right) u_j \bar{v}_j$$

By taking $\bar{v}_j = jh$, $j = 1, 2, \dots, n$, we get

$$(16) \quad 0 = u_n - u_0 = \frac{2-2\cos(kh)}{h^2} \sum_{j=1}^n u_j(jh)$$

Consequently,

$$(17) \quad \sum_{j=1}^n u_j(jh) = 0$$

If we assume $\sum_{j=1}^n u_j(jh)^l = 0$ for some l , by using the Lemma 2.1, we get

$$\begin{aligned} 0 &= \sum_{j=1}^n u_j(jh)^l \\ &= -\frac{1}{l+1} \sum_{j=1}^n \delta_x u_j(jh)^{l+1} \\ &= \frac{1}{(l+1)(l+2)} \sum_{j=1}^n \delta_x^2 u_j(jh)^{l+2} \\ &= -\frac{k^2}{(l+1)(l+2)} \sum_{j=1}^n \delta_x^2 u_j(jh)^{l+2} \end{aligned}$$

Thus,

$$\sum_{j=1}^n u_j(jh)^{l+2} = 0$$

and it follows by induction that

$$(18) \quad \sum_{j=1}^n u_j(jh)^l = 0, \quad l = 1, 3, 5, \dots$$

We now conclude that

$$(19) \quad u_j = 0, \quad j = 1, 2, \dots, n$$

2.2. Two-dimensional problem. Next, we consider a two-dimensional Helmholtz equation,

$$(20) \quad -U_{xx}(x, y) - U_{yy}(x, y) - k^2U(x, y) = 0$$

The standard second-order five-point finite difference scheme for

$$U_{xx}(x, y) + U_{yy}(x, y)$$

is given by

$$(21) \quad \frac{U(x+h, y) + U(x-h, y) - 4U(x, y) + U(x, y+h) + U(x, y-h)}{h^2}.$$

Due to the existence of the incident angles and the cross derivative terms such as U_{xxyy} and U_{xxyyyy} appearing in the two-dimensional problem, it is not straightforward to extend the novel difference scheme from one-dimensional to two-dimensional Helmholtz equations. However, for a planar wave solution, Lambe et al. [12] considered a clever way to resolve the difficulty.

For $U(x, y) = e^{i(k_1x+k_2y)}$ with $(k_1, k_2) = (k \cos \theta, k \sin \theta)$, a direct computation gives

$$(22) \quad \begin{aligned} &U(x+h, y) + U(x-h, y) + U(x, y+h) + U(x, y-h) \\ &= 2(\cos(k_1h) + \cos(k_2h))U(x, y). \end{aligned}$$

The problem now becomes to seek an optimal ω , such that

$$(23) \quad 2(\cos(k_1h) + \cos(k_2h)) - (\omega - k^2h^2) \approx 0.$$

By minimizing the average over all angles, the value of ω is given by

$$(24) \quad \omega = 4J_0(kh) + (kh)^2,$$

where $J_0(kh) = \frac{1}{\pi} \int_0^\pi \cos(kh \sin(\theta)) d\theta$.

Thus, the new finite difference scheme for a two-dimensional equation is given by

$$(25) \quad -U(x+h, y) - U(x-h, y) + 4J_0(kh)U(x, y) - U(x, y+h) - U(x, y-h) = 0$$

Adopting the idea for the boundary points and extending to the radiation condition, the new finite difference approximations for $\frac{\partial U}{\partial x} = ik_1U$ and $\frac{\partial U}{\partial y} = ik_2U$ are given by

$$(26) \quad U(x+h, y) - 2i\sin(k_1h)U(x, y) - U(x-h, y) = 0,$$

and

$$(27) \quad U(x, y+h) - 2i\sin(k_2h)U(x, y) - U(x, y-h) = 0.$$

To treat the terms $\sin(k_1h)$ and $\sin(k_2h)$, we can apply similar procedure for dealing with $\cos(k_1h)$ and $\cos(k_2h)$ in the interior domain. For the two-dimensional problem, we have the following uniqueness theorem.

THEOREM 2.2 (Uniqueness of the discretized solution). *By the novel finite difference schemes (25), (26) and (27), the discretized system has a unique solution under the condition $\max(k_1h, k_2h) < \pi$.*

Proof: Assuming there are two solutions w and v , let $u = w - v$, then u satisfies the equation

$$(28) \quad \begin{cases} -\frac{u_{i+1,j}+u_{i-1,j}-\omega u_{i,j}+u_{i,j-1}+u_{i,j+1}}{h^2} - k^2 u_{i,j} = 0, & i, j = 1, 2, \dots, n \\ u_{0,j} = u_{j,0} = 0, & j = 1, 2, \dots, n \\ u_{n+1,j} - 2i \sin(k_1 h) u_{n,j} - u_{n-1,j} = 0, & j = 1, 2, \dots, n \\ u_{j,n+1} - 2i \sin(k_2 h) u_{j,n} - u_{j,n-1} = 0, & j = 1, 2, \dots, n \end{cases}$$

Using the standard notation, equation (28) can be rewritten as

$$\begin{cases} -\delta_x^2 u_{i,j} - \delta_y^2 u_{i,j} - \left(\frac{4-\omega}{h^2} + k^2\right) u_{i,j} = 0, & i, j = 1, 2, \dots, n \\ u_{0,j} = u_{j,0} = 0, & j = 1, 2, \dots, n \\ u_{n+1,j} - u_{n,j} = i \sin(k_1 h) u_{n,j} + (1 - \cos(k_1 h)) u_{n,j}, & j = 1, 2, \dots, n \\ u_{j,n+1} - u_{j,n} = i \sin(k_2 h) u_{j,n} + (1 - \cos(k_2 h)) u_{j,n}, & j = 1, 2, \dots, n \end{cases}$$

By multiplying the equation by $\bar{v}_{i,j}$ and summing-up the equation for i, j from 1 to n , we get

$$\sum_{i=1}^n \sum_{j=1}^n (-\delta_x^2 u_{i,j} - \delta_y^2 u_{i,j}) \bar{v}_{i,j} - \sum_{i=1}^n \sum_{j=1}^n \left(\frac{4-\omega}{h^2} + k^2\right) u_{i,j} \bar{v}_{i,j} = 0.$$

Next, the discrete integration by parts is applied to δ_x^2 and δ_y^2 . For $\sum_{i=1}^n \sum_{j=1}^n -\delta_x^2$, we

have

$$\begin{aligned} h^2 \sum_{i=1}^n \sum_{j=1}^n (-\delta_x^2 u_{i,j}) \bar{v}_{i,j} &= - \sum_{i=1}^n \sum_{j=1}^n (u_{i-1,j} - u_{i,j} - (u_{i,j} - u_{i+1,j})) \bar{v}_{i,j} \\ &= - \sum_{i=1}^n \sum_{j=1}^n (u_{i-1,j} - u_{i,j}) \bar{v}_{i,j} + \sum_{k=2}^{n+1} \sum_{j=1}^n (u_{k-1,j} - u_{k,j}) \bar{v}_{k-1,j} \\ &= - \sum_{i=2}^n \sum_{j=1}^n (u_{i-1,j} - u_{i,j}) \bar{v}_{i,j} - \sum_{j=1}^n (u_{0,j} - u_{1,j}) \bar{v}_{1,j} \\ &\quad + \sum_{i=2}^n \sum_{j=1}^n (u_{k-1,j} - u_{k,j}) \bar{v}_{k-1,j} + \sum_{j=1}^n (u_{n,j} - u_{n+1,j}) \bar{v}_{n,j} \\ &= h^2 \sum_{i=1}^n \sum_{j=1}^n \delta_x u_{i,j} \delta_x \bar{v}_{i,j} - h \sum_{j=1}^n \delta_x u_{n,j} \bar{v}_{n,j} \end{aligned}$$

Hence,

$$(29) \quad \sum_{i=1}^n \sum_{j=1}^n (-\delta_x^2 u_{i,j}) \bar{v}_{i,j} = \sum_{i=1}^n \sum_{j=1}^n \delta_x u_{i,j} \delta_x \bar{v}_{i,j} - \frac{1}{h} \sum_{j=1}^n \delta_x u_{n,j} \bar{v}_{n,j}.$$

Similarly, for $\sum_{i=1}^n \sum_{j=1}^n -\delta_y^2$,

$$(30) \quad \sum_{i=1}^n \sum_{j=1}^n (-\delta_y^2 u_{i,j}) \bar{v}_{i,j} = \sum_{i=1}^n \sum_{j=1}^n \delta_y u_{i,j} \delta_y \bar{v}_{i,j} - \frac{1}{h} \sum_{i=1}^n \delta_y u_{i,n} \bar{v}_{i,n}.$$

Consequently,

$$\sum_{i=1}^n \sum_{j=1}^n \delta_x u_{i,j} \delta_x \bar{v}_{i,j} - \frac{1}{h} \sum_{j=1}^n \delta_x u_{n,j} \bar{v}_{n,j} + \sum_{i=1}^n \sum_{j=1}^n \delta_y u_{i,j} \delta_y \bar{v}_{i,j}$$

$$(31) \quad -\frac{1}{h} \sum_{i=1}^n \delta_y u_{i,n} \bar{v}_{i,n} - \sum_{i=1}^n \sum_{j=1}^n \left(\frac{4-\omega}{h^2} + k^2 \right) u_{i,j} \bar{v}_{i,j} = 0.$$

Taking $\bar{v}_{i,j} = \bar{u}_{i,j}$, $i, j = 1, 2, \dots, n$ in equation(31) and using the boundary schemes, we get

$$(32) \quad \begin{aligned} & \sum_{i=1}^n \sum_{j=1}^n \delta_x u_{i,j} \delta_x \bar{u}_{i,j} + \sum_{i=1}^n \sum_{j=1}^n \delta_y u_{i,j} \delta_y \bar{u}_{i,j} - \sum_{i=1}^n \sum_{j=1}^n \left(\frac{4-\omega}{h^2} + k^2 \right) u_{i,j} \bar{u}_{i,j} \\ & - \frac{1}{h^2} \sum_{j=1}^n \left((1 - \cos(k_1 h)) u_{n,j} + i \sin(k_1 h) u_{n,j} \right) \bar{u}_{n,j} \\ & - \frac{1}{h^2} \sum_{j=1}^n \left((1 - \cos(k_2 h)) u_{j,n} + i \sin(k_2 h) u_{j,n} \right) \bar{u}_{j,n} = 0. \end{aligned}$$

Since the right-hand side of equation (32) is real, it follows that

$$(33) \quad \sum_{j=1}^n \left(\sin(k_1 h) u_{n,j} \bar{u}_{n,j} + \sin(k_2 h) u_{j,n} \bar{u}_{j,n} \right) = 0.$$

With $\max(k_1 h, k_2 h) < \pi$, $\sin(k_1 h) > 0$ and $\sin(k_2 h) > 0$. Hence,

$$(34) \quad u_{n,j} = u_{j,n} = 0, \quad j = 1, 2, \dots, n$$

Substituting equation(34) into equation(31), it yields

$$(35) \quad \sum_{i=1}^n \sum_{j=1}^n \delta_x u_{i,j} \delta_x \bar{v}_{i,j} + \sum_{i=1}^n \sum_{j=1}^n \delta_y u_{i,j} \delta_y \bar{v}_{i,j} = \sum_{i=1}^n \sum_{j=1}^n \left(\frac{4-\omega}{h^2} + k^2 \right) u_{i,j} \bar{v}_{i,j}.$$

If we take $\bar{v}_{i,j} = \left(\frac{j-1}{n} + i \right) h$, $i, j = 1, 2, \dots, n-1$ and $\bar{v}_{i,j} = 0$, $i, j = 0$ or n in equation(35), we have

$$\begin{aligned} & \sum_{i=1}^n \sum_{j=1}^n \delta_x u_{i,j} \delta_x \bar{v}_{i,j} = \sum_{i=1}^n \sum_{j=1}^n \delta_x u_{i,j} \delta_x \left(\left(\frac{j-1}{n} + i \right) h \right) \\ & = \sum_{i=1}^n \sum_{j=1}^n \delta_x u_{i,j} = \sum_{j=1}^n (u_{n,j} - u_{0,j}) = 0. \end{aligned}$$

Therefore,

$$(36) \quad \sum_{i=1}^n \sum_{j=1}^n \delta_x u_{i,j} \delta_x \bar{v}_{i,j} = 0.$$

Similarly, we can show that

$$(37) \quad \sum_{i=1}^n \sum_{j=1}^n \delta_y u_{i,j} \delta_y \bar{v}_{i,j} = 0.$$

Substituting equation(36) and equation(37) into equation(35), it gives

$$\sum_{i=1}^n \sum_{j=1}^n \left(\frac{4-\omega}{h^2} + k^2 \right) u_{i,j} \left(\left(\frac{j-1}{n} + i \right) h \right) = 0,$$

with $\omega \neq 4 + k^2 h^2$, we have

$$(38) \quad \sum_{i=1}^n \sum_{j=1}^n \left(\frac{j-1}{n} + i \right) h u_{i,j} = 0.$$

Now, assume for some positive integer l ,

$$(39) \quad \sum_{i=1}^n \sum_{j=1}^n \left(\left(\frac{j-1}{n} + i \right) h \right)^l u_{i,j} = 0.$$

Then, by Lemma 2.1, we have

$$\begin{aligned} 0 &= \sum_{i=1}^n \sum_{j=1}^n \left(\left(\frac{j-1}{n} + i \right) h \right)^l u_{i,j} \\ &= -\frac{1}{l+1} \sum_{i=1}^n \sum_{j=1}^n \left(\left(\frac{j-1}{n} + i \right) h \right)^{l+1} \delta_x u_{i,j} \\ (40) \quad &= \frac{1}{(l+1)(l+2)} \sum_{i=1}^n \sum_{j=1}^n \left(\left(\frac{j-1}{n} + i \right) h \right)^{l+2} \delta_x^2 u_{i,j}. \end{aligned}$$

Similarly,

$$(41) \quad \frac{1}{(l+1)(l+2)} \sum_{i=1}^n \sum_{j=1}^n \left(\left(\frac{j-1}{n} + i \right) h \right)^{l+2} \delta_y^2 u_{i,j} = 0.$$

Using the finite difference equation and equations (40) and (41), we can easily verify

$$\sum_{i=1}^n \sum_{j=1}^n \left(\left(\frac{j-1}{n} + i \right) h \right)^{l+2} u_{i,j} = 0.$$

It follows by mathematical induction that for $l = 1, 3, 5, \dots$

$$(42) \quad \sum_{i=1}^n \sum_{j=1}^n \left(\left(\frac{j-1}{n} + i \right) h \right)^l u_{i,j} = 0.$$

We conclude that

$$(43) \quad u_{i,j} = 0, \text{ for } i, j = 1, 2, \dots, n$$

Remark: If the value of θ in $J_0(kh)$ (see equation(24)) is known, the exact solution can be computed numerically using the novel finite difference schemes. However, generally speaking, the value of θ is not available, and thus the optimal ω which depend on the incident angle θ can not be determined. It should be noted that unlike many high order methods such as the compact difference scheme or the spectral method, an attractive feature of the novel difference schemes is that exact numerical solution is achieved while the structure and the bandwidth of the corresponding matrix is the same as those derived from a second-order central difference scheme. Hence, the use of the novel difference schemes does not increase the complexity and the storage requirement for solving the resulting linear system.

3. Numerical simulations

To demonstrate the effectiveness of the novel finite difference schemes presented in the previous section, we carry out the following numerical simulations. Here, we consider two mathematical models, Mode 1 and Model 2, which have been studied in [4, 5, 17]. Let SFD and NFD denote the standard second-order central finite difference and the novel finite difference schemes applying to the interior points, respectively. To investigate the effect due to the radiation boundary condition, let SBC denote the use of the standard central difference scheme for the boundary

points and NBC denote the application of the new finite difference scheme for the boundary. The numerical error is defined in the discrete l_∞ norm,

$$E_\infty = \max_{i=1,\dots,n_x} \max_{j=1,\dots,n_y} |u_{i,j} - \bar{u}_{i,j}|,$$

where $u_{i,j}$ is the analytical solution and $\bar{u}_{i,j}$ is the computed numerical solution. Let n_x and n_y be the numbers of the grid points in the x- and y-direction.

One of the important factors in studying wave propagation problems numerically is the point per wavelength (PPW). In many engineering applications, it has been stated that PPW should be about 10 - 12 to ensure a reasonable computed solution. Since the wave length is defined by

$$(44) \quad \lambda = \frac{2\pi}{k},$$

dividing both sides by h , the value of PPW can be estimated by

$$(45) \quad PPW = \frac{\lambda}{h} = \frac{2\pi}{kh}.$$

The above equation indicates the importance of kh , and to ensure $PPW \sim 12$, we need $kh \sim 0.5$.

3.1. Model 1: Uniaxial Propagation of a Plane Wave. Consider a one-dimensional Helmholtz equation which models the propagation of a time-harmonic plane wave along the x-axis,

$$(46) \quad \begin{cases} -U_{xx} - k^2U = 0, & x \in (0, 1) \\ U(0) = 1, \\ U'(1) - ikU(1) = 0. \end{cases}$$

The exact solution for this problem is given by e^{ikx} . Using the finite difference approximations, the solution of the Helmholtz equation is obtained by solving the resulting system of linear difference equations

$$(47) \quad AU = b,$$

where the matrix A is tridiagonal and indefinite. For one-dimensional problems, the solution of the linear system is solved using a direct method.

TABLE 1. E_∞ for SFD and NFD with $h=0.01$

		SBC		NBC	
kh	k	SFD	NFD	SFD	NFD
0.1	10	0.0048	0.0017	0.0040	4.29e-14
0.3	30	0.1106	0.0149	0.1148	1.26e-14
0.5	50	0.5371	0.0428	0.5274	9.55e-15
0.7	70	1.3487	0.0823	1.3856	1.28e-14
1	100	1.9998	0.1792	2.0216	5.60e-15
1.5	150	2.4932	0.3928	2.0043	5.66e-16

In Table 1 and Table 2, we compare the performance using the standard central difference and the new finite difference schemes when the step-size h and the wavenumber k is fixed. From the results presented here, we observe that the NFD provides more accurate numerical solutions for all cases. When h is fixed, the error increases as k increases. However, for a fixed k , the error is reduced when h

TABLE 2. E_∞ for SFD and NFD with $k=50$

		SBC		NBC	
kh	h	SFD	NFD	SFD	NFD
2.0	0.04	1.8617	1.0581	1.8623	5.6e-16
1.0	0.02	1.8112	0.1858	1.8740	2.9e-15
0.5	0.01	0.5371	0.0428	0.5274	9.6e-15
0.25	0.005	0.1300	0.0105	0.1314	4.3e-14
0.125	0.0025	0.0322	0.0026	0.0328	1.5e-13

is decreasing. Even though the radiation boundary is imposed only at one point $x=1$, the overall numerical solution is strongly depended on whether the boundary condition is computed by SBC or NBC. When the new finite difference schemes are employed for the interior and boundary points (i.e., using NFD and NBC), the exact solution is obtained. It is important to note that using NFD and NBC, the exact solution can be obtained even when $kh > 1$.

TABLE 3. E_∞ for SFD and NFD with NBC and $kh = 0.5$

k	10	50	100	200	500
h	0.05	0.01	0.005	0.0025	0.001
SFD	0.1229	0.5371	1.0353	1.7602	2.0263
NFD	1.77e-15	9.56e-15	1.93e-15	3.65e-14	9.35e-13

Table 3 compares the numerical solutions of SFD and NFD using NBC and with $kh = 0.5$. Recall that using $kh = 0.5$, it provides about 12 points per wavelength. It clearly demonstrates that with $PPW \sim 12$, the standard difference scheme can not resolve the oscillatory behavior for cases at high wavenumbers.

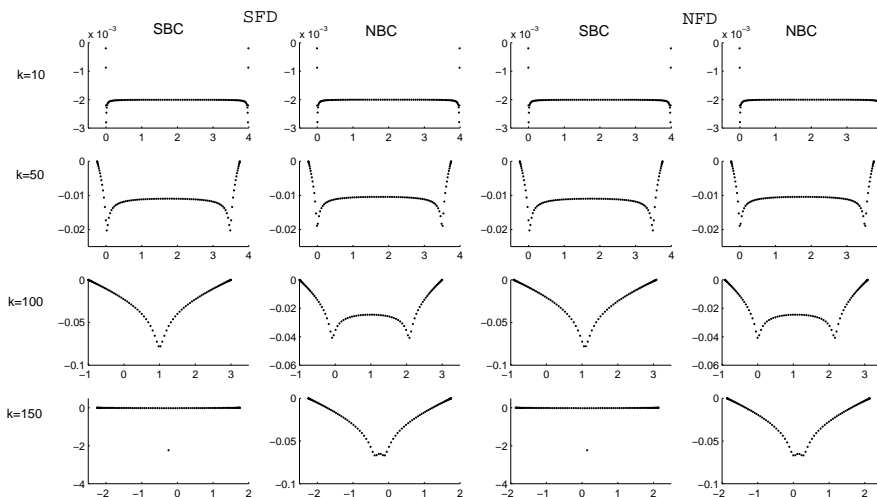


FIGURE 1. The eigenvalues for linear system based on SFD and NFD with boundary schemes using SBC and NBC

The importance of applying NBC can be revealed from the eigenvalue distribution displayed in Figure 1. Here, $h = 0.01$, $k = 10, 50, 100$ and 150 , and hence,

$kh = 0.1, 0.5, 1$ and 1.5 . The profiles of the eigenvalue plots are similar when kh is small. However, for large value of kh , the eigenvalue profiles are significantly difference when the radiation boundary condition is approximated by SBC or NBC. It is of interest to note the eigenvalue distribution of SFD and NFD is similar when the boundary condition is approximated by the same type of difference approximations. A careful investigation shows that the main difference is due to the shifting as displayed in the eigenvalue plots, and this is verified that the large error in the numerical solutions between SFD and NFD is indeed due to the phase shift of the wave solution.

From the numerical simulations presented for the one-dimensional problems, it is obvious that solving the Helmholtz equation numerically for cases with high wavenumbers are more difficult than those with low wavenumbers. Since problems with high wavenumbers are ill-conditioned, it is naturally to expect that the condition numbers of the resulting linear system increases as k increases.

TABLE 4. Condition numbers with $h = 0.01$

scheme	k=5	k=25	k=50	k=100	k=125
SFD	5080.1	1016.9	503.4	229.6	252.3
NFD	5081.5	1014.5	499.8	243.2	199.0

Let the condition number be defined as $\lambda_{max}(A^H A)/\lambda_{min}(A^H A)$. For $h = 0.01$, Table 4 lists the condition numbers corresponding to the wavenumber k in the range of 5 to 125. The values of the condition numbers for SFD and NFD are similar, but it decreases from 5000 to about 200 as the wavenumber increases from 5 to 125. This unexpected results can be explained by the fact that as k increases the smallest eigenvalue actually is moving away from zero as shown in Table 5. Thus in solving the Helmholtz equation numerically, small condition number does not imply the problem is well-conditioned.

TABLE 5. Min and Max eigenvalues of with $h = 0.01$

k	λ_{min}					λ_{max}				
	5	25	50	100	125	5	25	50	100	125
SFD	6.2e-7	1.5e-5	5.6e-5	2.0e-4	1.7e-4	16.0	15.5	14.1	10.7	10.7
NFD	6.2e-7	1.5e-5	5.7e-5	1.8e-4	2.2e-4	16.0	15.5	14.2	10.3	8.8

3.2. Model 2: Propagation of Plane Waves. We now consider a two-dimensional Helmholtz equation on a unit square $\Omega = (0, 1) \times (0, 1)$ with radiation boundary conditions on two sides and the Dirichlet boundary conditions on the remaining boundaries. This problem is formulated as:

$$(48) \quad \begin{cases} \Delta U + k^2 U = 0, & (x, y) \in \Omega \\ U(x, y) = f_1(x), & y = 0 \\ U(x, y) = f_2(y), & x = 0 \\ \frac{\partial U}{\partial y} = ik_2 U, & y = 1 \\ \frac{\partial U}{\partial x} = ik_1 U, & x = 1 \end{cases}$$

The exact solution $U = e^{i(k_1 x + k_2 y)}$ where $(k_1, k_2) = (k \cos \theta, k \sin \theta)$, f_1 and f_2 are determined such that the exact solution is a given plane wave.

Recall that the new difference schemes are given as

$$\begin{cases} -u_{i+1,j} - u_{i-1,j} + 4J_0(kh)u_{i,j} - u_{i,j+1} - u_{i,j-1} = 0, & i, j = 1, 2, \dots, n \\ u_{n+1,j} - 2i \sin(k_1 h)u_{n,j} - u_{n-1,j} = 0, & j = 1, 2, \dots, n \\ u_{j,n+1} - 2i \sin(k_2 h)u_{j,n} - u_{j,n-1} = 0, & j = 1, 2, \dots, n \end{cases}$$

with Dirichlet conditions on $x = 0$ and $y = 0$.

In the numerical simulation, $J_0(kh)$ is computed using the formula given the previous section and exact boundary conditions are imposed using NBC. As a test case, we consider $\theta = \frac{\pi}{4}$. The resulting system of difference equations has the same structure as those using the five-point difference formula. Since the matrix is usually large and sparse, the linear system is solved using the generalized minimal residual method GMRES(m) with $m=30$ and the stopping condition is based on the residual norm satisfying the tolerance $< 10^{-6}$. GMRES is a powerful iterative scheme, and it is capable of solving indefinite linear systems. The details of GMRES algorithms can be found in [1].

TABLE 6. E_∞ and $J_0(kh)$ for $h = 0.02$

kh	k	E_∞		$J_0(kh)$	
		SFD	NFD	$[0, \pi]$	Exact θ
0.8485	$30\sqrt{2}$	1.70661	3.21431	3.645368	3.648019
0.7071	$25\sqrt{2}$	2.60665	0.79162	3.752593	3.753879
0.5657	$20\sqrt{2}$	0.71042	0.25167	3.841065	3.841593
0.4243	$15\sqrt{2}$	0.20008	0.10524	3.910337	3.910505
0.2828	$10\sqrt{2}$	0.13488	0.07627	3.960067	3.960099
0.1414	$5\sqrt{2}$	0.04299	0.00349	3.990004	3.990006

In Table 6, we report the error norm E_∞ using the SFD and NFD for various value of k and the step-size is kept at $h = 0.02$. Although the numerical solutions using NFD are more accurate compared to those based on SFD for most cases, we note that NFD does not produce exact numerical solutions as in one-dimensional cases. This is due to the fact that in calculation of the matrix coefficient involved $J_0(kh)$, the exact angle of incident θ is not known. Hence, $J_0(kh)$ is actually computed by taking average of all angles in the range of $[0, \pi]$ in equation(24). Recall that in our test model $\theta = \frac{\pi}{4}$, and it has been verified numerically that instead of using the range $[0, \pi]$, NFD will produce more accurate numerical solution if $J_0(kh)$ is determined using the angle in the range $[\frac{\pi}{8}, \frac{3\pi}{8}]$. Moreover, when exact value of θ is employed, exact solution can be computed numerically. It should also mentioned when solving the resulting linear systems by GMRES for the test cases reported in Table 6, the residual norm is decreasing as the iteration is increased, and it will be terminated when the prescribed tolerance $< 10^{-6}$ is reached. However, the error norm could remain large for problems with high wavenumbers as reported in Table 6.

Thus for two-dimensional problems, the NFD is not effective unless information about the angle is known. In the following, assuming that the angle is in the range of $[0, \frac{\pi}{2}]$, we present an algorithm using nonlinear least-squares to improve the estimate for θ .

Least-square Algorithm:

1 Determine the coefficients of the linear system $Ax = b$ by calculating $J_0(kh)$ in $[0, \frac{\pi}{2}]$

- 2 Solve the system by GMRES and let the solution be x_{temp} ,
- 3 Take partial data from x_{temp} (we take the two lines besides the Dirichlet boundaries in this study) and form the least square function

$$f(x, \theta) = \sum_{j=1}^m (A(j) - x(j, \theta))^2,$$

where $A(j)$ are the data from x_{temp} and $x(j, \theta)$ are the exact solution of plane wave ($e^{k(x \cos(\theta) + y \sin(\theta))}$) with parameter θ .

- 4 Estimate θ using a nonlinear least-square such as the Levenberg-Marquardt algorithm. Using different initial approximations in Step 4, we determine θ_1 and θ_2 .
- 5 Update the coefficients of the system $Ax = b$ by recomputing $J_0(kh)$ in $[\theta_1, \theta_2]$
- 6 Repeat steps 2-5 until θ converges.

Remark: When applying the nonlinear least-square method to estimate θ , we need an initial approximation for the Levenberg-Marquardt algorithm. Suppose several initial approximations θ_i are used, then we may have several possible solutions for θ . Now, let θ_1 and θ_2 be selected such that they are in the range of $[0, \frac{\pi}{2}]$. Other solutions which are outside the range will be ignored.

TABLE 7. Estimating θ_1 and θ_2 in least-square process for $h = 1/200$ and $k = 60\sqrt{2}$

step	interval	initial data						
		$\frac{\pi}{16}$	$\frac{2\pi}{16}$	$\frac{3\pi}{16}$	$\frac{4\pi}{16}$	$\frac{5\pi}{16}$	$\frac{6\pi}{16}$	$\frac{7\pi}{16}$
1	$[0, \pi/2]$	10.21	1.245	0.097	0.785	1.474	0.326	8.636
2	$[0.097, 1.474]$	-6.032	-5.370	1.245	0.785	0.326	6.941	7.196
3	$[0.326, 1.245]$	-5.205	1.551	0.658	0.785	0.913	0.020	7.069
4	$[0.658, 0.913]$	0.568	0.785	0.785	0.785	0.785	0.785	1.003
5	$[0.785, 0.785]$	0.785	0.785	0.785	0.785	0.785	0.785	0.785

To illustrate the use of the above algorithm, we consider a two-dimensional problem, and let the step-size in both x- and y- direction be $h = 1/200$ and the wavenumber $k = 60\sqrt{2}$, thus $kh = 0.424$. Starting with $[0, \pi/2]$, and let the initial approximations be $\frac{i\pi}{16}$, $i=1,2,\dots,7$, the estimated θ are reported in Table 7. From the solutions of the nonlinear least-square, it is obvious that 10.21 and 8.636 are outside $[0, \pi/2]$; and for the remaining five acceptable solutions, they are in the range of $[0.097, 1.474]$. Thus, we let $\theta_1 = 0.097$ and $\theta_2 = 1.474$. By repeating the process, and we note that after 5 steps, θ is converging to 0.785, and recall that the the exact angle is $\pi/4=0.7853975$.

TABLE 8. Estimated θ_1 and θ_2 for various k and $h = 1/200$

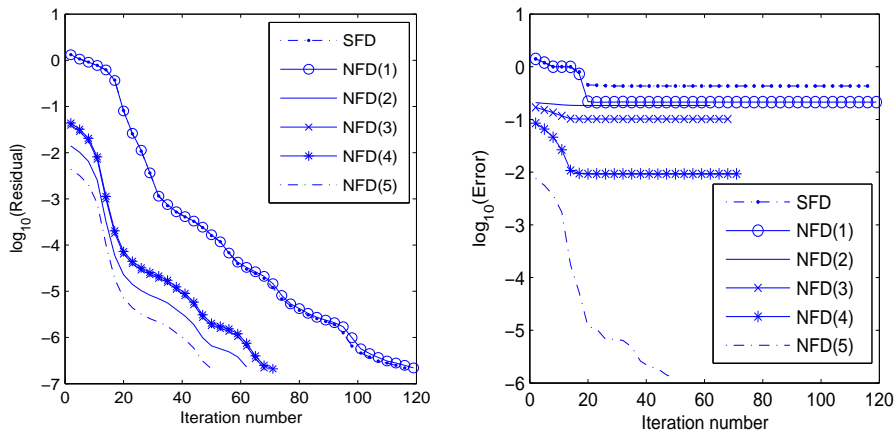
step	$k = 60\sqrt{2}$	$k = 200$	$k = 300$
1	$0, \frac{\pi}{2}$	$0, \frac{\pi}{2}$	$0, \frac{\pi}{2}$
2	0.09722302, 1.47357316	0.19743746, 1.37335858	0.39838750, 1.17240883
3	0.32611235, 1.24468426	0.61556731, 0.95522921	0.49217431, 1.07862160
4	0.65759956, 0.91319670	0.68625372, 0.88454261	0.61416985, 0.95662640
5	0.78537393, 0.78542241	0.73077586, 0.84002050	0.78539812, 0.78539821
6	—	0.78538820, 0.78540815	—

The least-square algorithm can be incorporated with the NFD scheme, so that the solution of the Helmholtz equation is obtained through solving a sequence of linear systems. At each step, the angle is estimated. When θ converges to a constant value, very accurate numerical solutions are obtained. This procedure has been tested for large wavenumbers and for cases where $kh > 1$. In Table 8, we report the estimated θ_1 and θ_2 for wavenumbers $k = 60\sqrt{2}$, 200, 300, respectively. Since $h = 1/200$, $kh = 0.424$, 1.0 and 1.5. It is noted that even when kh is large and > 1 , the number of steps in the least-square estimations does not increase significantly. When the values of k and kh are small, rapid convergent is observed. Table 9 shows the corresponding error norms in using the combined NFD and the least-square. It confirms that when θ is accurately estimated, NFD produces accurate numerical solution. The accuracy can be further improved if we adjust the stopping condition in the GMRES iterations.

TABLE 9. NFD Error norm at various steps with $h = 1/200$

step	E_∞		
	$k = 60\sqrt{2}$	k=200	k=300
1	0.21359839	1.91769813	2.02601222
2	0.18440064	1.66355707	2.01655199
3	0.10184648	0.22103007	1.76463131
4	0.00925021	0.07679778	0.77773616
5	0.00000120	0.02345849	0.00000121
6	—	0.00000220	—

The performance for solving two-dimensional problems using SFD and NFD with least-square (NFD-LS) for $k = 60\sqrt{2}$ and $k = 300$ are shown in Fig. 2 and Fig. 3. We clearly observe that even when the error norm remains large, the residual norm in the GMRES is decreasing as the number of iterations increased. Hence, we may obtain poor numerical solution by checking only the residual norm. The power of the NFD-LS is clearly demonstrated in Fig. 3.

FIGURE 2. Error and Residual norms for SFD and NFD-LS for $h = 1/200$ and $k = 60\sqrt{2}$

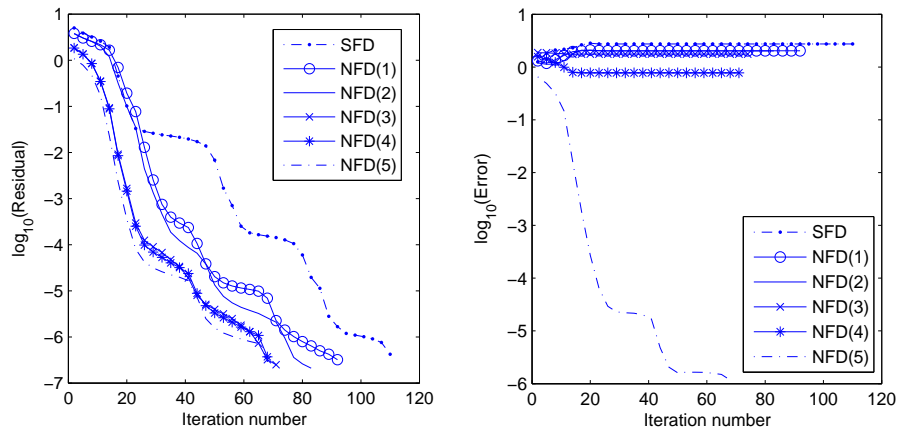


FIGURE 3. Error and Residual norms for SFD and NFD-LS for $h = 1/200$ and $k = 300$

4. Conclusion

Novel finite difference schemes for solving the Helmholtz equation are presented in this study. It has been shown that the new difference schemes satisfy the Helmholtz equation and the radiation boundary conditions exactly. Since there is no truncation error, exact numerical solutions are expected for problems at any wavenumber. The most attractive features of this method are that it can be applied to high frequency cases without the common requirement of using a fine step size. Moreover, the high accurate numerical solutions are obtained while the resulting linear system has the same simple sparse structure as those derived from the standard second order central difference approximation. The proofs of the uniqueness of the discretized systems resulting for one- and two-dimensional Helmholtz equations are given. Numerical simulations are carried out to verify exact numerical solutions are obtained for one-dimensional problems at any wavenumber. For a two-dimensional problem, the new finite difference scheme requires good estimate of the angle. A simple least-square algorithm is proposed so that the angle and hence the accuracy of the Helmholtz solutions can be improved iteratively. Incorporating the new difference schemes and the least-square method, the solution of a two-dimensional Helmholtz equation can be accurately and efficiently computed. The power of this technique has been demonstrated by comparing the performance of the standard difference and the new difference schemes to two test models considered in this paper. It is of interest to extend the applications to other models, and to investigate the effectiveness when solving the Helmholtz equation with a perfectly matched layer method.

References

- [1] O. Axelsson. Iterative Solution Methods, Cambridge University Press, Cambridge, New York, Oakleigh, 1994
- [2] J. Autrique and F. Magoulés. Numerical analysis of a coupled finite- infinite element method for exterior helmholtz problems. *Journal of Computational Acoustics*, 14:21–43, 2006.
- [3] I. Babuška, F. Ihlenburg, T. Strouboulis, and S. K. Gangaraj. A posteriori error estimation for nite element solutions of helmholtz equation. part i: The quality of local indicators and estimators. *International Journal For Numerical Methods In Engineering*, 40:3443–3462, 1997.

- [4] I. Babuška and S. A. Sauter. Is the pollution effect of the fem avoidable for the helmholtz equation considering high wave. *SIAM J. Numer. Anal.*, 34:2392–2423, 1997.
- [5] G. Bao, G. W. Wei, and S. Zhao. Numerical solution of the helmholtz equation with high wavenumbers. *Int. J. Numer. Meth. Engng*, 59:389–408, 2004.
- [6] J. P. Berenger. A perfectly matched layer for the absorption of electromagnetic waves. *Journal of Computational Physics*, 114:185–200, 1994.
- [7] B. Engquist and A. Majda. Absorbing boundary conditions for the numerical simulation of waves. *Math. Comp*, 31:629–651, 1977.
- [8] C. J. Gittelsohn, R. Hiptmair, I. Perugia. Plane wave discontinuous galerkin methods: analysis of the h-version, *Mathematical Modelling and Numerical Analysis*, 43, 297–331, 2009
- [9] I. Harari and F. Magoulés. Numerical investigations of stabilized finite element computations for acoustics. *Wave Motion*, 39:339–349, 2004.
- [10] I. Harari and E. Turkel. Accurate finite difference methods for time-harmonic wave propagation. *Journal of Computational Physics*, 119:252–270, 1995
- [11] F. Ihlenburg and I. Babuška. Finite element solution of the helmholtz equation with high wave number part i: The h-version of the FEM. *Computers & Mathematics with Applications*, 30:9–37, 1995.
- [12] L. A. Lambe, R. Luczak, and J. W. Nehrbass. A new finite difference method for the helmholtz equation using symbolic computation. *International Journal of Computational Engineering Science*, 4:121–144, 2003.
- [13] M. Nabavia, M.H. K. Siddiqui, and J. Dargahi. A new 9-point sixth-order accurate compact finite-difference method for the helmholtz equation. *Journal of Sound and Vibration*, 307:972–982, 2007.
- [14] I. Singer and E. Turkel. High-order finite difference methods for the helmholtz equation. *Comput. Methods Appl. Mech. Engrg.*, 163:343–358, 1998.
- [15] I. Singer and E. Turkel. Sixth order accurate finite difference schemes for the helmholtz equation. *J. Comput. Acoustics*, 14:339–351, 2006.
- [16] G. Sutmann. Compact finite difference schemes of sixth order for the helmholtz equation. *Journal of Computational and Applied Mathematics*, 203:15–31, 2007.
- [17] I. Tsukerman. A class of difference schemes with flexible local approximation. *Journal of Computational Physics*, 211:659–699, 2006.

Department of Mathematical and Statistical Sciences, University of Alberta, Edmonton, Alberta, T6G 2G1, Canada

E-mail: yaushu.wong@ualberta.ca